Acta Med. Okayama, 2021
Vol. 75, No. 2, pp. 153-167

Acta Medica Okayama
http://escholarship.lib.okayama-u.ac.jp/amo/

Original Article

Lactoferrin-like Immunoreactivity in Distinct Neuronal Populations in the Mouse Central Nervous System

Shigeyoshi Shimaoka[a], Hitomi Hamaoka[a], Junji Inoue[a], Masato Asanuma[b], Ikuo Tooyama[c], and Yoichi Kondo[a]*

[a]Department of Anatomy and Cell Biology, Division of Life Sciences, Osaka Medical and Pharmaceutical University, Takatsuki, Osaka 569-8686, Japan, [b]Department of Medical Neurobiology, Okayama University Graduate School of Medicine, Dentistry and Pharmaceutical Sciences, Okayama 700-8558, Japan, [c]Molecular Neuroscience Research Center, Shiga University of Medical Science, Otsu 520-2192, Japan

Lactoferrin (Lf) is an iron-binding glycoprotein mainly found in exocrine secretions and the secondary granules of neutrophils. In the central nervous system (CNS), expression of the Lf protein has been reported in the lesions of some neurodegenerative disorders such as Alzheimer's disease, Parkinson's disease, and amyotrophic lateral sclerosis, as well as in the aged brain. Lf is primarily considered an iron chelator, protecting cells from potentially toxic iron or iron-requiring microorganisms. Other biological functions of Lf include immunomodulation and transcriptional regulation. However, the roles of Lf in the CNS have yet to be fully clarified. In this study, we raised an antiserum against mouse Lf and investigated the immunohistochemical localization of Lf-like immunoreactivity (Lf-LI) throughout the CNS of adult mice. Lf-LI was found in some neuronal populations throughout the CNS. Intense labeling was found in neurons in the olfactory systems, hypothalamic nuclei, entorhinal cortex, and a variety of brainstem nuclei. This study provides detailed information on the Lf-LI distribution in the CNS, and the findings should promote further understanding of both the physiological and pathological significance of Lf in the CNS.

Key words: lactoferrin, immunohistochemistry, brain mapping

Lactoferrin (Lf) is an 80-kDa iron-binding glycoprotein that is mainly found in exocrine secretions, such as breast milk [1,2], and in the secondary granules of neutrophils [3].

The affinity of Lf for iron is far stronger than that of transferrin, the closest relative of Lf in the transferrin family of proteins [4]. Thus, Lf is considered an iron chelator rather than a transporter. In regard to its function, Lf was first postulated to act as an iron chelator to protect breast-fed infants from enteric pathogens that require iron [5]. In this context, it is likely that Lf in the secondary granules of neutrophils sequesters toxic iron released from destroyed tissue and keep leukocytes safe at the site of inflammation. Lf is also one of the components of neutrophil extracellular traps (NETs), which are a fibrous network of DNA released from the nuclei of neutrophils, and appears to participate in the killing of bacteria trapped on NETs [6].

Apart from such roles in innate immunity, Lf possesses multiple functions in the regulation of the immune system and acts as a transcription factor in the regulation of protein synthesis [7-9]. For example, Lf enhances natural killer cell activity [10] and inhibits lipopolysaccharide-mediated production of interleukin-1, interleukin-6, and tumor necrosis factor-alpha

Received October 17, 2020; accepted November 6, 2020.
*Corresponding author. Phone: +81-72-684-6411; Fax: +81-72-684-6511
E-mail: konchan@ompu.ac.jp (Y. Kondo)

Conflict of Interest Disclosures: No potential conflict of interest relevant to this article was reported.

[11, 12]. Unlike other members of the transferrin family, Lf has a strongly basic region near its N-terminus, which binds specific DNA sequences [13], and thus acts as a novel transcription factor. Lf was found to down-regulate granulocyte macrophage colony-stimulating factor promoter in interleukin-1 beta-stimulated fibroblasts [14].

In the CNS, it has been reported that Lf is expressed in a variety of neurodegenerative conditions, such as Alzheimer's disease [15, 16], Parkinson's disease [17], amyotrophic lateral sclerosis, and Pick's disease [15]. Lf has been immunohistochemically demonstrated to localize mainly in neurons affected by these neurodegenerative lesions. The high binding affinity of Lf to ferric ions leads us to speculate that Lf may protect neurons from oxygen free radicals by chelating potentially toxic iron in the brain. However, because of the many putative functions of Lf described above, the role of Lf in the CNS is yet to be determined.

To clarify the physiological distribution of Lf in the CNS, we raised an antiserum against a synthetic oligopeptide specific for mouse Lf and determined the immunohistochemical localization of lactoferrin-like immunoreactivity (Lf-LI) in the mouse CNS. We show that Lf is found in a variety of neuronal populations throughout the CNS of ten-week-old mice. This is the first report to describe the detailed distribution of Lf-LI in the healthy CNS.

Materials and Methods

All animal experiments were approved by the institutional Review Board of the Osaka Medical College (approval nos. 30113 and 2019-113) and were performed according to procedures outlined in the Guide for the Animal Care and Use of Laboratory Animals of the Osaka Medical College.

Production of an antiserum to mouse lactoferrin. A synthetic oligopeptide specific for mouse Lf (RWQNEMRKVGGPPLSC) was prepared, conjugated with bovine serum albumin (Peptide Institute Inc., Osaka, Japan) and then used in the immunization of rabbits to raise a polyclonal antibody against the synthetic peptide. This oligopeptide corresponds to amino acid residues 39-54 of mouse Lf, which are in the first domain of the N-terminal lobe. This amino acid sequence has no homology to mouse transferrin. Based on the three-dimensional structure of human Lf, this mouse sequence is surface-exposed and contains a transition from an alpha-helix to a beta-strand structure [18].

Western blot analysis. Male ICR mice (10 weeks of age) were used in this study. The animals (n = 3) were euthanized with sodium pentobarbital (120 mg/kg, i.p.) and then decapitated. The whole brains were homogenized in three volumes of ice-cold 20 mM Tris-HCl (pH 7.6) containing 150 mM NaCl, 1% NP-40, 0.1% CHAPS, 0.1% SDS and protease inhibitor cocktail (Complete™; Roche, Basel, Switzerland), and incubated on ice for 30 min. The homogenate was centrifuged at 12,000 rpm for 30 min at 4°C. The supernatant was removed and again centrifuged at 12,000 rpm for 30 min at 4°C. The supernatant collected as total cell lysate was used for western blot analysis.

Ten-μg protein samples were electrophoresed on 10% sodium dodecyl sulfate-polyacrylamide gel (SDS-PAGE) and transferred to a nitrocellulose membrane (Hybond™-ECL; Amersham, Buckinghamshire, UK). Equivalent protein loading was confirmed by staining the membrane with 0.1% Ponceau S in 5% acetate. The membrane was blocked with 3% bovine serum albumin (fraction V; Sigma) in 20 mM Tris-HCl (pH 7.6) containing 150 mM NaCl and 0.1% Tween 20 (TBS-T) for 1 h at room temperature (RT) and further incubated overnight with anti-Lf antiserum (1 : 100,000) in TBS-T at 4°C. As a negative control experiment, anti-Lf antiserum was replaced with pre-immune serum (1 : 100,000) or the antiserum that had been adsorbed overnight at 4°C with 10 mM of the synthetic Lf oligopeptide. The membrane was washed with TBS-T, reacted with HRP-linked anti-rabbit immunoglobulin (1 : 5,000; Amersham) in TBS-T, and washed again with PBS-T. Immunoreactive bands were visualized by enhanced chemiluminescence (ECL, Amersham).

Tissue preparation for immunohistochemistry. The animals (n = 3) were euthanized with sodium pentobarbital (120 mg/kg, i.p.) and perfused transcardially with 10 mM phosphate-buffered saline (pH 7.2) followed by a fixative containing 4% paraformaldehyde (PFA), 0.35% glutaraldehyde, and 0.2% picric acid in 100 mM phosphate buffer (pH 7.4). The brains and spinal cords were removed and post-fixed for approximately 24 h in the same fixative excluding glutaraldehyde, cryoprotected in 15% sucrose in 100 mM phosphate buffer for 48 h, snap frozen with powdered dry ice, and cut coronally on a cryostat at 20 μm. Sections

were stored in 100 mM phosphate-buffered saline containing 0.3% triton X-100 (PBS-T, pH 7.4) and subjected to immunohistochemical staining using the free-floating method [19, 20]. The above procedures were carried out at 4°C.

Immunohistochemistry. Free-floating sections at each 100-μm interval throughout the rostral-caudal axis of the brain and spinal cord were immunolabelled for Lf. Endogenous peroxidase activity in the sections was quenched with 0.5% H_2O_2 in PBS-T for 30 min. The sections were first incubated for 10 days with anti-Lf serum (1 : 100,000), for 24 h with biotinylated anti-rabbit IgG (diluted 1 : 1,000; Vector Laboratories, Burlingame, CA, USA), and for 1 h with the avidin-biotin peroxidase complex (diluted 1 : 2,000; Vector Laboratories). All antibody dilutions and washing of sections were performed with PBS-T. Peroxidation activity was visualized with 0.02% 3, 3'-diaminobenzidine (DAB; Katayama Chemical, Osaka, Japan), 0.0045% H_2O_2, and 0.3% nickel ammonium sulphate in 50 mM Tris-HCl buffer (pH 7.6). The stained sections were mounted on glass slides coated with silane (APS-01; Matsunami Glass Industry, Kishiwada, Japan), air-dried, dehydrated, and cover slipped. Images were digitally recorded with a DS-Ri1 camera (Nikon, Tokyo) on a Nikon Eclipse 80i light microscope (Nikon).

For immunohistochemical controls, primary antiserum was replaced with pre-immune rabbit serum at the same dilution (1 : 100,000). In addition, anti-Lf antiserum that had been previously adsorbed with 10 mM of the synthetic antigen peptide for 24 h at 4°C was used as the control antiserum. As a positive control, 10-μm cryosections mounted on the glass slides were prepared from the uteri of perfusion-fixed mice (10 weeks old; n = 2). Briefly, the slides were incubated for 30 min with 1% H_2O_2 in PBS-T, for 30 min with 5% normal goat serum in PBS-T, overnight at 4°C with anti-Lf antiserum (1 : 5,000) or pre-immune serum (1 : 5,000), for 1 h with biotinylated goat anti-rabbit IgG (diluted 1 : 100; Vector Laboratories), and for 30 min with the avidin-biotin peroxidase complex (diluted 1 : 200; Vector Laboratories). The immunoreactivities were visualized by incubating the slides with DAB plus nickel ammonium sulphate as described above. We photographed these control slides using a Keyence BZ-X700 microscope equipped with phase contrast objective lenses (Keyence, Osaka, Japan) to outline negatively stained sections.

Results

Specificity of antiserum against Lf. The polyclonal antiserum was tested for specificity using western blotting of mouse brain homogenates. This antiserum detected a single band with an estimated molecular weight of approximately 80 kDa (Fig. 1A, lane 1). Controls

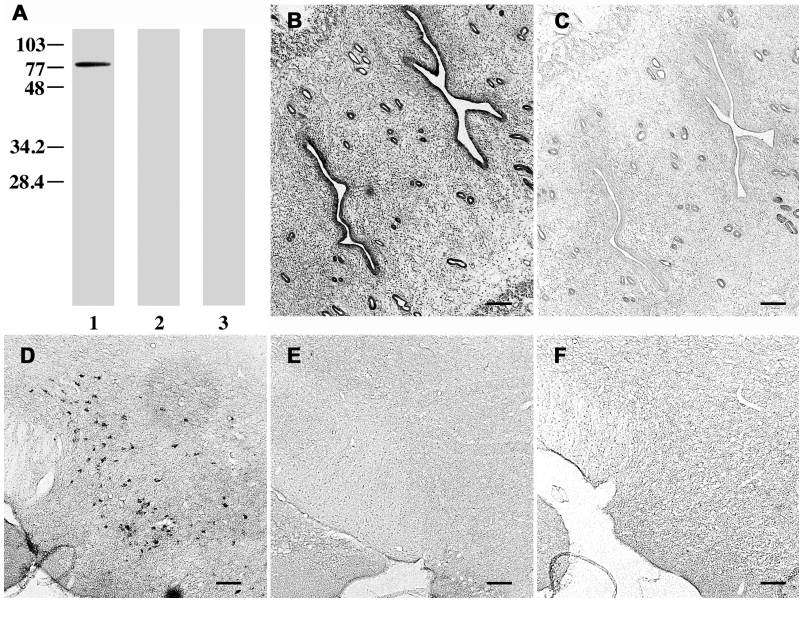

Fig. 1 The specificity of anti-lactoferrin serum. **A**, Western blot analysis of mouse brain homogenate. Equivalent protein loading was confirmed by staining the membrane with 0.1% Ponceau S in 5% acetate. The antiserum (diluted 1 : 100,000) detected a single band at 80 kDa (A, lane 1). Controls using either pre-immune serum (A, lane 2) or antiserum previously adsorbed with 10 mM of the synthetic peptide antigen (RWQNEMRKVGGPPLSC) used for immunization (A, lane 3) did not reveal any bands. Molecular sizes are indicated at left (in kDa); **B**, **C**, Photomicrographs of positive control immunolabeling of the mouse endometrial glands with the anti-lactoferrin antiserum (B) and with pre-immune serum (C); **D**–**F**, Immunolabeling of the brain with anti-lactoferrin antiserum (D) and negative control staining with pre-immune serum (E) and the pre-adsorbed antiserum described above (F). Phase contrast images are shown in panels B–F. Scale bars = 100 μm.

using either pre-immune serum (Fig. 1A, lane 2) or antiserum previously adsorbed with 10 mM of the synthetic peptide antigen (RWQNEMRKVGGPPLSC) used for immunization (Fig. 1A, lane 3) did not show any bands.

Immunohistochemical staining of the mouse uterus with the antiserum revealed Lf-LI in the epithelium of the endometrial glands (Fig. 1B), whereas the pre-immune serum did not yield such immunoreactivity (Fig. 1C). Lf-LI was similarly observed in the mouse CNS (Fig. 1D). Substituting the antiserum with the pre-immune serum or pre-adsorbed anti-serum completely abolished Lf-LI (Fig. 1E, F).

Distribution of Lf-like immunoreactivity in the mouse brain and spinal cord. Lf-LI was observed in a certain population of neurons throughout the rostral-caudal extent of the brain and spinal cord. The reaction product in neurons appeared to occur on the surface of cells and in the cytoplasm. In some brain regions, dendritic or axonal processes were also visible. Maps of positive neuronal somata are presented in Fig. 2 with 18 schematic drawings of coronal sections, corresponding to the atlas of the mouse brain by Hof *et al.* [21], and in Fig. 10A with a schematic drawing of the cervical spinal cord.

Telencephalon. In the main olfactory bulb, Lf-LI

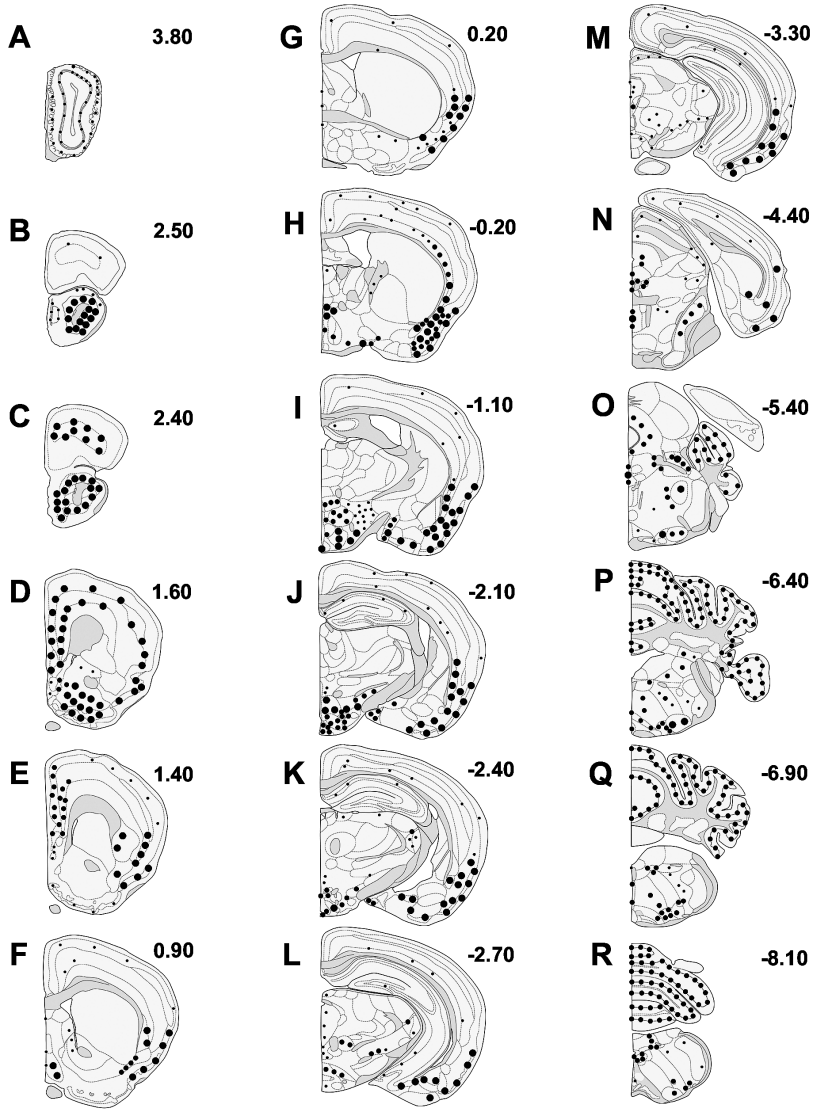

Fig. 2 Mapping of neuronal lactoferrin-like immunoreactivity in coronal sections of the mouse brain. Lactoferrin-like immunoreactivity is depicted by dots that represent both the number and distribution of labeled cells. For the intensity of signals, see Table 1. Small dots = 1–5 labeled cells; medium dots = 6–10 labeled cells; large dots = approximately 50 labeled cells. The number indicates the anteroposterior distance of the panel from the bregma.

was found in both the cytoplasm and dendrites of mitral cells, tufted cells, and periglomerular cells (Fig. 2A and 3A, B). Lf-LI in dendrites was prominent in the external plexiform layer and to a lesser degree in the glomeruli (Fig. 3A, B). In the accessory olfactory bulb, scattered neurons in the mitral cell layer were clearly positive for Lf-LI (Fig. 3A, C, D), and the external plexiform layer and glomerular layer showed diffuse and fibrous staining (Fig. 1A, D). Many positive neurons were seen in the anterior olfactory nuclei and tenia tecta (Fig. 2B-D and 3E).

The lateral stripe of the striatum contained weakly immunoreactive but concentrated small-sized neurons (Fig. 2F-H and 4A). The piriform cortex contained positive neurons of various sizes according to its layer structure (Fig. 2D-K and 4A). Moderate staining was seen in the tightly packed small pyramidal cells in layer II, and relatively dense staining was seen in the medium to large-sized pyramidal cells scattered in layers III-IV. Other paleocortices, including the agranular insular cortex (Fig. 2E-H, 4B), lateral entorhinal cortex (Fig. 2J-N and 4C), and perirhinal cortex (Fig. 2L, M and 4D), had a number of medium-sized neurons showing neuronal somata and proximal axons and dendrites positive for Lf-LI. No positive structures were seen in the hippocampal formation except for occasional horizontal cells in the stratum oriens in the CA1 (Fig. 4E) and other areas (Fig. 2I-M). Unlike the paleocortex, the neocortex contained only a few positive non-pyramidal cells scattered throughout the layer structure (Fig. 2F-N and 4F). Among the neocortices, the primary and secondary motor cortex were the only exception, where a number of moderately positive neurons were observed (Fig. 2B-E). Lf-LI was not found in the caudoputamen (Fig. 2E-J).

Many, but not all, neurons in the nuclei of the horizontal- and vertical-limb of the diagonal band showed intense Lf-LI (Fig. 2F and 5A). Lf-positive neurons were packed in the supraoptic nucleus (Fig. 2H and 5B). The medial preoptic area, including the medial, lateral, and

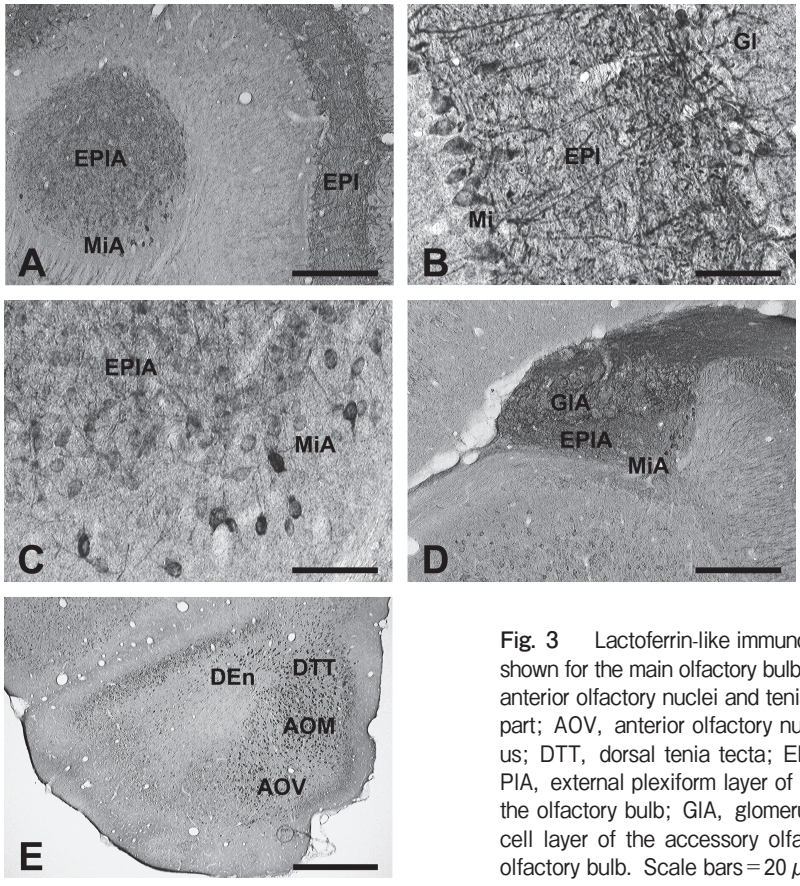

Fig. 3 Lactoferrin-like immunoreactivity in the mouse olfactory system. Results are shown for the main olfactory bulb (**A**, **B**), accessory olfactory bulb (**A**, **C**, and **D**), and anterior olfactory nuclei and tenia tecta (**E**). AOM, anterior olfactory nucleus, medial part; AOV, anterior olfactory nucleus, ventral part; DEn, dorsal endopiriform nucleus; DTT, dorsal tenia tecta; EPI, external plexiform layer of the olfactory bulb; EPIA, external plexiform layer of the accessory olfactory bulb; GI, glomerular layer of the olfactory bulb; GIA, glomerular layer of the accessory olfactory bulb; Mi, mitral cell layer of the accessory olfactory bulb; MiA, mitral cell layer of the accessory olfactory bulb. Scale bars = 20 μm for (A, D); 5 μm for (B, C) and 50 μm for (E).

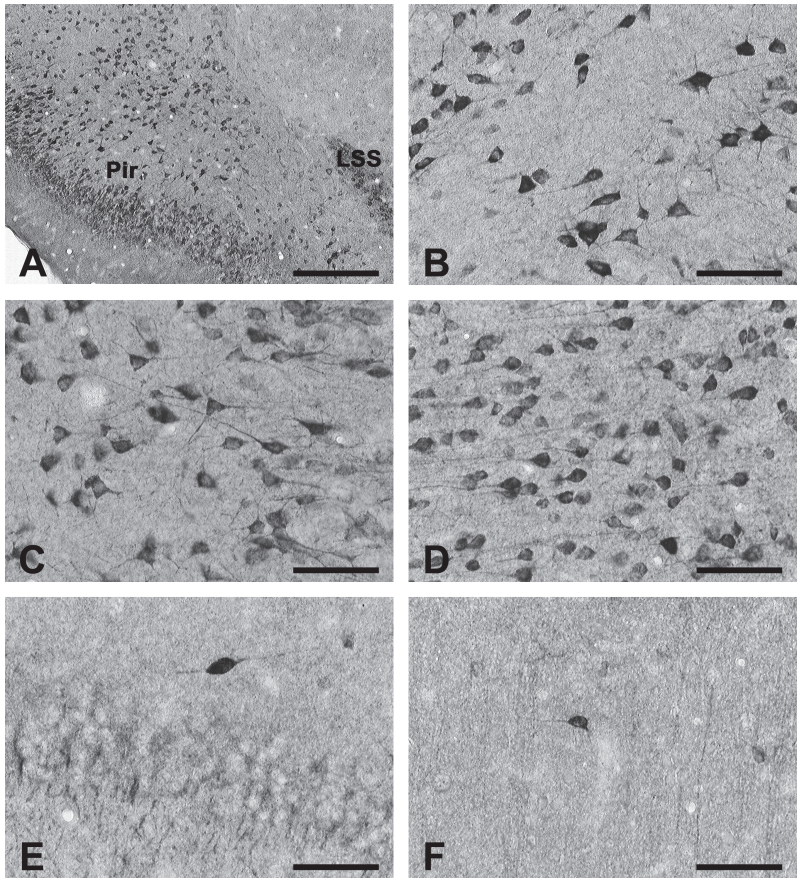

Fig. 4 Neuronal lactoferrin-like immunoreactivity in the piriform cortex and lateral stripe of the striatum (A), posterior part of the agranular insular cortex (B), lateral entorhinal cortex (C), perirhinal cortex (D), stratum oriens of the hippocampal CA1 area (E), and layer I of the frontal cortex (F). LSS, lateral stripe of the striatum; Pir, piriform cortex. Scale bars = 20 μm for (A) and 5 μm for (B–F).

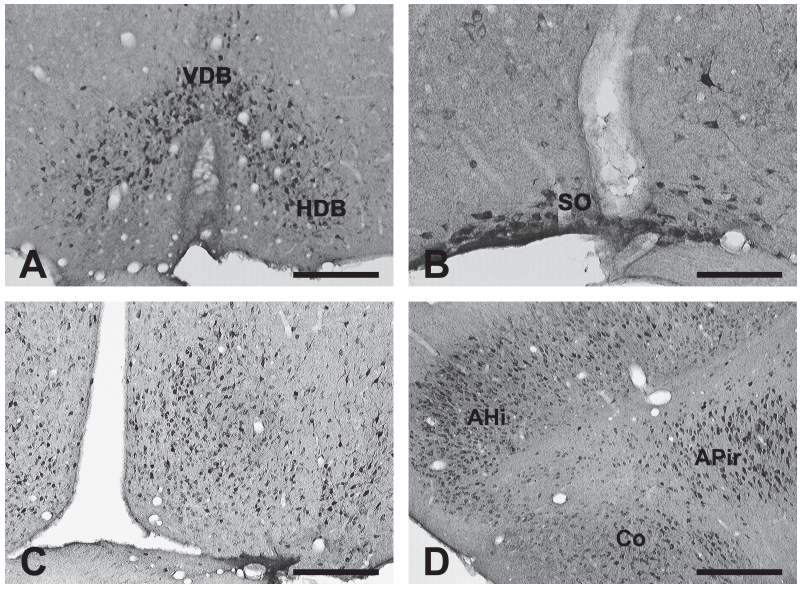

Fig. 5 Lactoferrin-like immunoreactivity in the telencephalon. Results are shown for nuclei of the horizontal- and vertical-limb of the diagonal band (A), the supraoptic nucleus (B), the medial preoptic nucleus (C), and the amygdalohippocampal area, cortical amygdaloid nucleus, and amygdalopiriform transition area (D). AHi, amygdalohippocampal area; APir, amygdalopiriform transition area; Co, cortical amygdaloid nucleus; HDB, nucleus of the horizontal limb of the diagonal band; SO, supra optic nucleus; VDB, nucleus of the vertical limb of the diagonal band. Scale bars = 20 μm for (A, C, D) and 10 μm for (B).

central part of the medial preoptic nuclei, was abundant in medium-sized positive neurons with moderate to strong staining intensity (Fig. 2G, H and 5C). A number of neurons stained with moderate to strong intensity were found in the amygdalohippocampal area, cortical amygdaloid nucleus, and amygdalopiriform transition area (Fig. 2I-M and 5D).

Diencephalon. Lf-LI was most prominent in a series of hypothalamic nuclei in the CNS. Medium-sized positive neurons were concentrated in the anterior parvicellular part of the paraventricular hypothalamic nucleus, and some larger neurons with intense staining were scattered around the nucleus (Fig. 2H, I and 6A). The dorsomedial hypothalamic nucleus contained multipolar neurons with intensely stained neuronal somata and dendrites, while in the ventromedial hypothalamic nucleus, positive neurons were more frequent but had less staining intensity (Fig. 2J and 6B). The medial part of the arcuate nucleus comprised small-sized positive neurons and Lf-LI was confined to the neuronal somata and proximal processes (Fig. 2I-K and 6C). The lateral hypothalamic area showed large-sized positive neurons with strong intensity (Fig. 2I-K and 6D). Medium-sized positive neurons were diffusely scattered in the posterior hypothalamic area (Fig. 6E). Among thalamic structures, only the intergeniculate leaf had a concentrated population of positive neurons (Fig. 2K, L; photographs not shown).

Mesencephalon. Significant Lf-LI was not present in the substantia nigra, and positive neurons were found medial and dorsal to the substantia nigra pars compacta (Fig. 2L, M and 7A). Although the neuronal somata in the superior colliculus showed only faint positive staining, Lf-LI was found in the fibrous network in the zonal layer, superficial gray, and optic nerve layer (Fig. 7B). In the periaqueductal gray, positive neurons were scattered and somewhat dense in the lateral periaqueductal gray (Fig. 2M, N and 7C). The Edinger-Westphal nucleus had strong Lf-LI in the large-sized neurons (Fig. 2M and 7C). Large-sized neurons in the

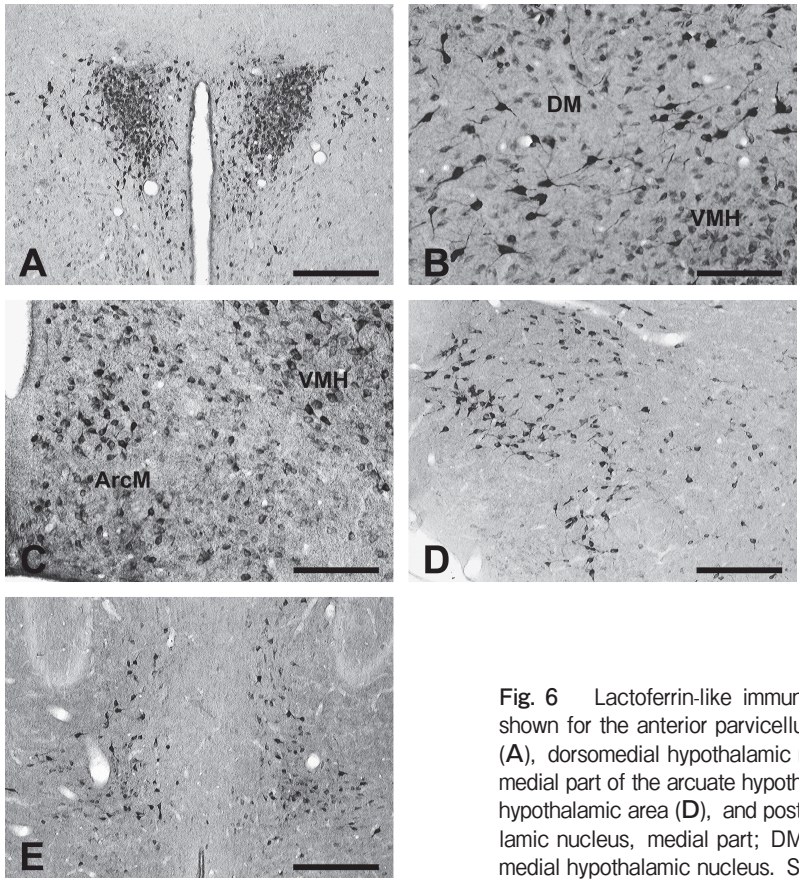

Fig. 6 Lactoferrin-like immunoreactivity in the hypothalamic areas. Results are shown for the anterior parvicellular part of the paraventricular hypothalamic nucleus (**A**), dorsomedial hypothalamic nucleus and ventromedial hypothalamic nucleus (**B**), medial part of the arcuate hypothalamic nucleus and ventromedial nucleus (**C**), lateral hypothalamic area (**D**), and posterior hypothalamic area (**E**). ArcM, arcuate hypothalamic nucleus, medial part; DM, dorsomedial hypothalamic nucleus; VMH, ventromedial hypothalamic nucleus. Scale bars = 20 μm for (A, D, E) and 10 μm for (B, C).

oculomotor nucleus showed light Lf-LI (Fig. 7C). In the dorsal raphe nuclei, medium-sized neurons with a mostly bipolar morphology showed moderate to strong Lf-LI in the dorsal (Fig. 7D), ventral, and ventromedial regions (Fig. 2N). Moderate to strong Lf-LI was found extensively but not densely in the supramammillary nucleus (Fig. 2K, L and 7E). The nucleus of the brachium inferior colliculus contained occasional neurons with intense Lf-LI (Fig. 2N and 7F). Moderately positive neurons with small round or bipolar morphology were seen in the paralemniscal nucleus (Fig. 2N and 7G).

Pons and medulla. Lf-LI was present in a moderate population of cells in the superior vestibular nucleus and genu of the facial nerve (Fig. 2P and 8A). The facial nucleus (Fig. 2P and 8B), lateral superior olive, and superior paraolivary nucleus (Fig. 2O and 8C) contained moderately positive neurons. The lateral paragigantocellular nucleus (Fig. 2P, Q and 8B), gigantocellular reticular nucleus (Fig. 2P, Q and 8D), and gigantocellular reticular nucleus, alpha part (Fig. 2P and 8E) showed moderate to strong Lf-LI in large-sized multipolar neurons. Positive neurons in the ambiguus nucleus were tightly packed (Fig. 2Q and 8F). In the mesencephalic trigeminal nucleus, positive neurons

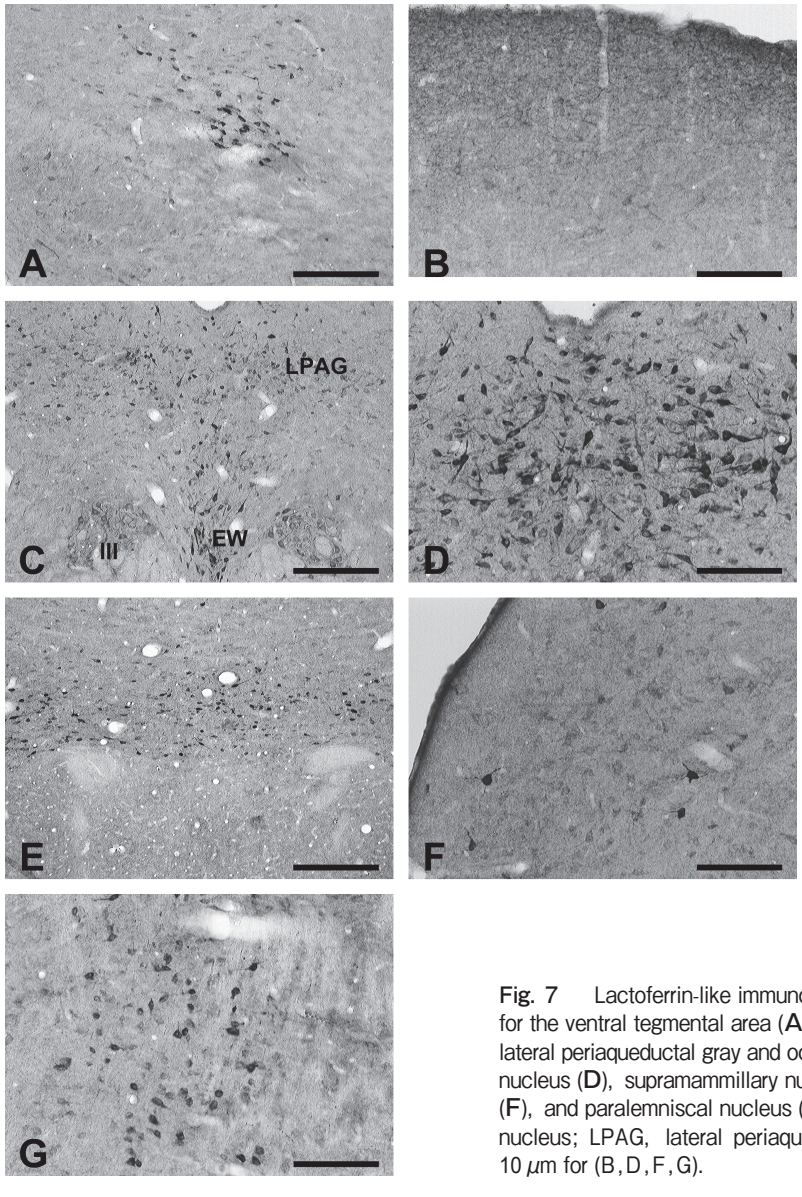

Fig. 7 Lactoferrin-like immunoreactivity in the mesencephalon. Results are shown for the ventral tegmental area (**A**), superior colliculus (**B**), Edinger-Westphal nucleus, lateral periaqueductal gray and oculomotor nucleus (**C**), dorsal part of the dorsal raphe nucleus (**D**), supramammillary nucleus (**E**), nucleus of the brachium inferior colliculus (**F**), and paralemniscal nucleus (**G**). III, oculomotor nucleus; EW, Edinger-Westphal nucleus; LPAG, lateral periaqueductal gray. Scale bars = 20 μm for (A, C, E) and 10 μm for (B, D, F, G).

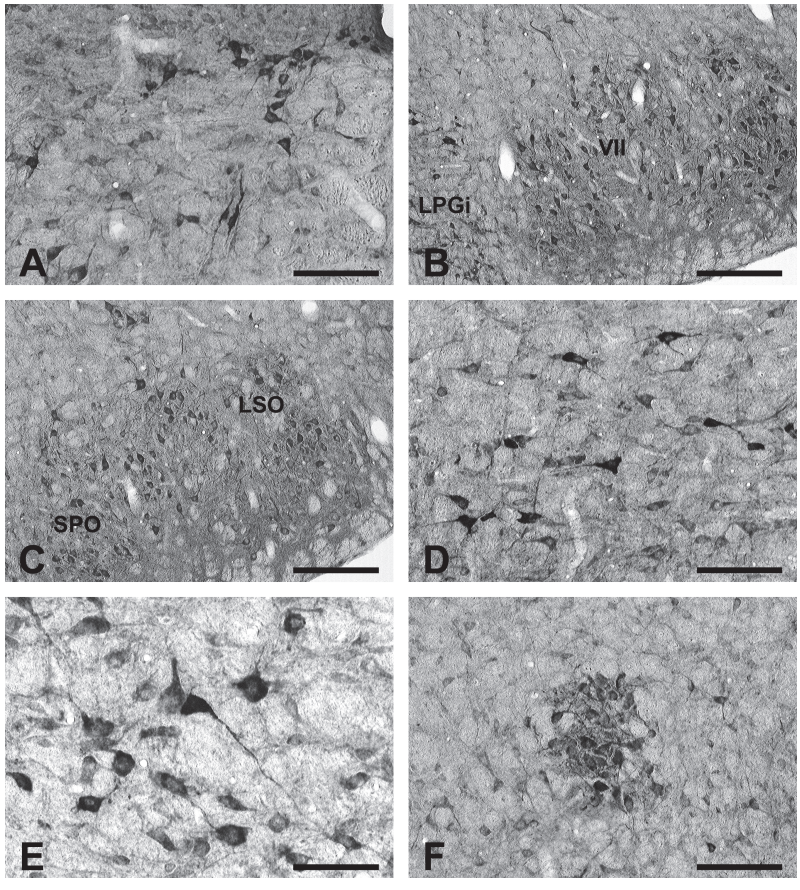

Fig. 8 Lactoferrin-like immunoreactivity in the pons. Results are shown for the genu of the facial nerve (**A**), facial nucleus and lateral paragigantocellular nucleus (**B**), lateral superior olive and superior paraolivary nucleus (**C**), gigantocellular reticular nucleus (**D**), alpha part of the gigantocellular reticular nucleus (**E**), and ambiguus nucleus (**F**). VII, facial nucleus; LSO, lateral superior olive; LPGi, lateral paragigantocellular nucleus; SPO, superior paraolivary nucleus. Scale bars = 10 μm for (A, D, F); 20 μm for (B, C) and 5 μm for (E).

had large and round morphology, and axons were also positive (Fig. 2O and 9A, B). Large-sized neurons with bipolar or multipolar morphology in the motor trigeminal nucleus were positive for Lf-LI together with their nerve fibers (Fig. 2O and 9A, C). There were scattered positive neurons in the central gray (Fig. 2O and 9A). Medium-sized positive neurons were found in the solitary tract nucleus including the intermediate, medial, ventral, and ventrolateral regions (Fig. 2Q, R and 9D). The dorsal motor nucleus of the vagus and hypoglossal nucleus showed light to moderate Lf-LI (Fig. 2Q and 9D). In the lateral reticular nucleus, most neurons showed weak to moderate Lf-LI with occasional strongly immunoreactive cells (Fig. 2R and 9E). The parvicellular reticular nucleus contained scattered positive neurons, but most of them showed strong Lf-LI (Fig. 2Q and 9F). Small-sized neurons in the rostroventrolateral reticular nucleus showed Lf-LI of variable intensity (Fig. 2Q, R and 9G).

Cerebellum. Clear Lf-LI was observed in the cytoplasm and proximal dendrites of the Purkinje cells (Fig. 2O-R and 9H).

Spinal cord. In the spinal cord, sporadic Lf-LI was seen in neurons in any layers of the gray matter (Fig. 10A-C). However, a number of large-sized motor neurons were conspicuous in layer IX with moderate immunoreactivity (Fig. 10D).

Discussion

The antiserum against a synthetic oligopeptide from mouse Lf detected a specific 80-kDa protein in mouse brain extract (Fig. 1A) and showed its immunoreactivity mainly in the somata of various neuronal populations throughout the rostrocaudal axis of the mouse CNS (Table 1 and Fig. 2). To our knowledge, this is the first report to describe the detailed distribution of Lf-LI in the normal CNS using a specific antiserum to mouse Lf.

Kawamata *et al.* [16] and Leveugle *et al.* [15] observed pathologic Lf-immunolabeling in neurofibril-

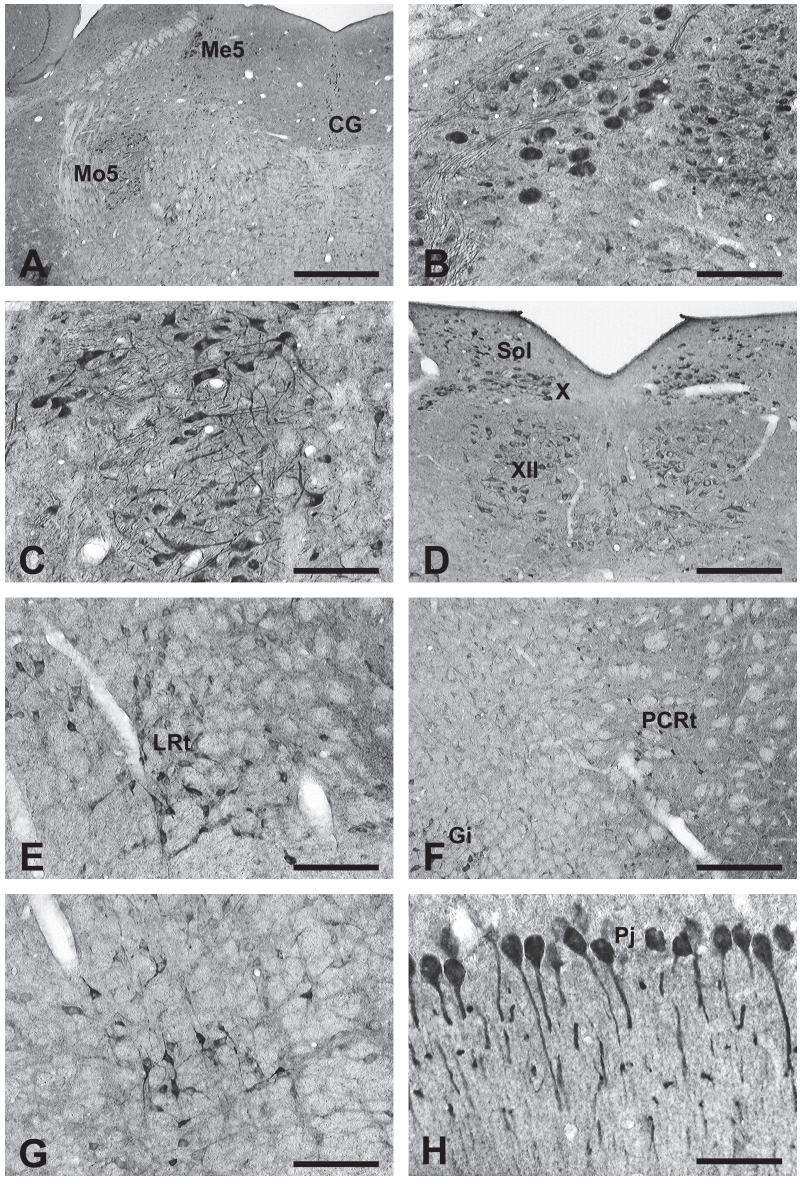

Fig. 9 Lactoferrin-like immunoreactivity in the medulla and cerebellum. Results are shown for the motor trigeminal nucleus, mesencephalic trigeminal nucleus, and central gray (**A**), mesencephalic trigeminal nucleus (**B**), motor trigeminal nucleus (**C**), nucleus of the solitary tract and hypoglossal nucleus (**D**), lateral reticular nucleus (**E**), parvicellular reticular nucleus (**F**), rostroventrolateral reticular nucleus (**G**), and Purkinje cells in the cerebellar cortex (**H**). X, dorsal motor nucleus of vagus; XII, hypoglossal nucleus; cc, central canal; CG, central (periaqueductal) gray; Gi, gigantocellular reticular nucleus; LRt, lateral reticular nucleus; Me5, mesencephalic trigeminal nucleus; Mo5, motor trigeminal nucleus; PCRt, parvicellular reticular nucleus; Pj, Purkinje cell layer of the cerebellum; Sol, solitary tract nucleus. Scale bars = 50 μm for (A); 10 μm for (B, C, E, G) 20 μm for (D, F), and 5 μm for (H).

lary tangles and senile plaques in the brains of patients with Alzheimer's disease, but reported that the brains of young control subjects were devoid of Lf staining, while the brains of elderly control subjects showed Lf labeling in some large pyramidal neurons in the prefrontal cortex [15] or in neurons in several areas, including the angular gyrus, hippocampus and entorhinal cortex [16]. It appears that neurons accumulate more Lf in particular brain areas with aging. Using our newly developed antibody, it will be possible to perform detailed investigations of chronological changes in Lf localization both in the developing and aging mouse brain. Lf labeling was also found in glial cells in the elderly brain [16], and in microglia in the prefrontal subcortical white matter of a patient with Alzheimer's disease [15]. In our study, glial staining for Lf was not found. Localization of Lf to glial cells may also be associated with aging via pathologic events such as inflammation, or simply associated with a species difference.

It is noteworthy that Lf-LI was scarce or weak in the majority of neocortices, and in the hippocampus, striatum, and substantia nigra, which are sites commonly affected by some neurodegenerative diseases and/or sites vulnerable to ischemia [22]. The significance of

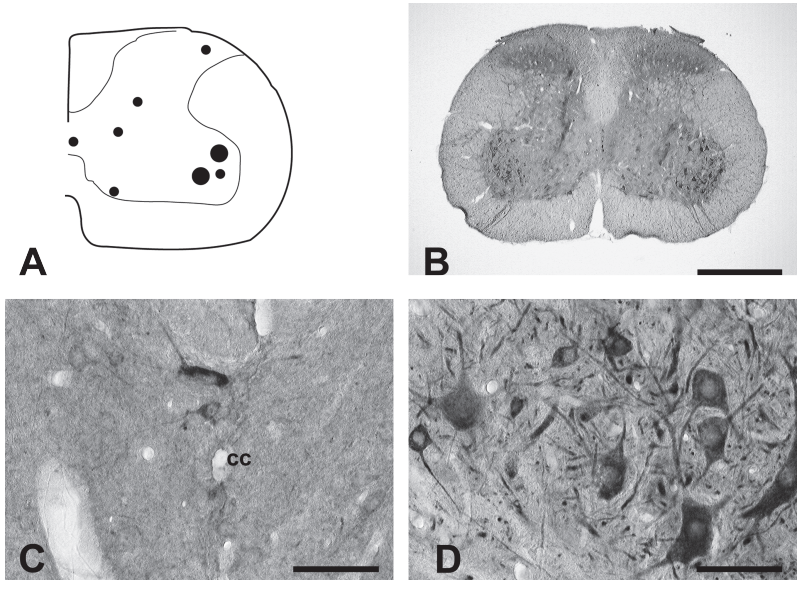

Fig. 10 Lactoferrin-like immunoreactivity in the spinal cord. Dots in the schematic drawing represent the mapping of the immunoreactivity in cervical spinal cord as comparable to Figure 2 (small dots = 1–5 labeled cells; medium dots = 6–10 labeled cells) (**A**). Photomicrographs of the immunolabeled cervical spinal cord: an entire cross-section view (**B**), layer X (**C**), and layer IX (**D**). cc, central canal. Scale bars = 50 μm for (B); 20 μm for (C) and 5 μm for (D).

such a lack of Lf is unclear at present. Since Lf has the potential to inhibit the formation of hydroxyl-radicals from superoxide and hydrogen peroxide by sequestering free iron [23], this observation allows us to speculate that Lf may confer protection against neuronal death by reducing oxidative stress, which is considered one of the potential causes of neuronal cell death in neurodegenerative diseases and cerebrovascular diseases. If that is the case, Lf could be of great therapeutic value, since orally administered Lf has been shown to improve neurocognitive function [24] and CNS inflammation [25] in animal models.

In this study, the most intense Lf-LI was found in a series of hypothalamic nuclei (Table 1, Fig. 6A-E). Indeed, preferential expression of the Lf receptor in the hypothalamus [26] may support the idea that Lf is involved in physiological functions in the hypothalamus. For instance, some hormonal feedback to the hypothalamus could be provided by Lf transported from the periphery. Indeed, an imperfect estrogen response element is present in the 5' flanking region of the Lf gene [27]; moreover, Lf gene expression is highly sensitive to estrogen in the mouse uterus, with the level of uterine Lf mRNA increasing up to 300-fold after estrogen administration [28]. In addition, estrogen replacement therapy has potentially beneficial effects on cognitive and mnemonic functions in patients with Alzheimer's disease [29, 30]. Thus, it is worth investigating whether any of those functions of estrogen are related to Lf accumulation in the CNS.

Although many different functions of Lf have been postulated (*e.g.*, iron chelator, immune modulator, transcription factor, antimicrobial property, and anticancer property [7, 8, 31]), the significance of the increased accumulation of Lf with age and in neurodegenerative disorders is not clear. In fact, it is not even known whether Lf is beneficial or detrimental in such disorders. A recent report, however, has shown that parkin controls iron homeostasis in cells through ubiquitylation of Lf, which might explain how dysfunction of parkin leads to Parkinson's disease [32]. Another in vitro study has suggested that Lf protects dopaminergic neurons by interacting with mitochondrial calcium homeostasis [33].

Receptors for Lf have been identified in different types of cells, including lymphocytes [34], platelets [35], small intestine cells [36], and epithelial cell lines from breast neoplasms [37]. As for the CNS, the presence of the Lf receptor in the blood brain barrier [38, 39] raises a question as to whether Lf is synthesized in neurons and/or transported from the plasma [40]. Fillebeen *et al.* [41, 42] showed the presence of Lf mRNA in the mouse brain using sensitive PCR, but failed to demonstrate its cellular localization using in situ hybridization, suggesting that the level of Lf mRNA is very low or that such sensitive PCR analysis might have detected the Lf mRNA of blood origin (*e.g.*, circulating neutrophils). Indeed, we found that Lf mRNA

Table 1 Distribution of lactoferrin-like immunoreactivity in the mouse CNS

Telencephalon	
Main olfactory bulb	
Glomerular layer	+
External plexiform layer (fibrous)	+
Mitral cell layer	+
Lateral olfactory tract	+
Dorsal lateral olfactory tract	+
Accessory olfactory bulb	
External plexiform layer (fibrous)	+
Mitral cell layer	+
Anterior olfactory nuclei (lateral, medial, dorsal, ventral, posterior, & external part)	++
Tenia tecta	
dorsal-	++
ventral-	+
Islands of Calleja	+
Piriform cortex	++
Dorsal endopiriform nucleus	++
Ventral endopiriform nucleus	+
Nucleus of the diagonal band (horizontal & vertical limb)	++
Medial preoptic area and nuclei (central, medial & lateral)	++
Primary motor cortex	+
Secondary motor cortex	+
Cingulate cortex, area 1	+
Prelimbic cortex	+
Granular insular cortex	+
Dorsal peduncular cortex	+
Agranular insular cortex	+
Entorhinal cortex	+
Lateral entorhinal cortex	+
Retrosplenial agranular cortex	+
Basal ganglia	
Lateral stripe of the striatum	+
Ventral pallidum	+
Amygdala	
Medial nuclei (anterodorsal, anteroventral, posterodorsal, & posteroventral part)	+
Anterior cortical nucleus	+
Posterolateral cortical nucleus	+
Posteromedial cortical nucleus	+
Basomedial nuclei (anterior & posterior part)	+
Basolateral nuclei (anterior & ventral part)	+
Bed nucleus of the accessory olfactory tract	+
Premammillary nuclei (dorsal and ventral part)	++
Amygdalohippocampal area (anterolateral & posteromedial part)	+
Amygdalopiriform transition area	++
Supraoptic nucleus	+++
Diencephalon	
Hypothalamus	
Paraventricular nuclei (dorsal cap, & anterior parvicellular, medial parvicellular, lateral magnocellular, posterior & ventral part)	++++
Periventricular nucleus	+
Ventromedial nuclei (anterior, central, dorsomedial & ventrolateral part)	+++
Arcuate nuclei	++
Anterior area (central and posterior part)	+
Dorsal area	+
Lateral area	+++
Posterior area	+
Magnocellular nucleus of the lateral hypothalamus	+++
Dorsomedial nuclei (dorsal, ventral & compact part)	++
Medial tuberal nucleus	++
Supramammillary nucleus	++
Tuber cinereum area	+
Retrochiasmatic area	+
Subincertal nucleus	+
Zona incerta	+
Thalamus	
Anteroventral nucleus	+
Paratenial nucleus	+
Subparafascicular nucleus	+
Submammillothalamic nucleus	+
Intergeniculate leaf	+
Prerubral field	++
Rostral interstitial nucleus of medial longitudinal fasciculus	+
Olivary pretectal nucleus	+
Ethmoid nucleus	+

Mesencephalon	
Superior colliculus (zonal, superficial gray & optic nerve layer)	++
Inferior colliculus	
Nucleus of the brachium	++
Medial geniculate nuclei (dorsal, medial & ventral part)	+
Tegmental nuclei	
Substantia nigra (lateral part)	++
Edinger-Westphal nucleus	++
Rostral linear nucleus of the raphe	++
Interpeduncular nuclei (rostral & lateral subnucleus)	++
Oculomotor nucleus	+
Pararubral nucleus	+
Red nucleus	+
Dorsal raphe nuclei (dorsal, ventral & ventrolateral part)	+++
Median raphe nucleus	+
Paratrochlear nucleus	+
Paralemniscal nucleus	+
Lateral periaqueductal gray	++
Raphe magnus nucleus	+
Raphe pallidus nucleus	+
Medial parabrachial nucleus	++
Mesencephalic trigeminal nucleus	+
Laterodorsal tegmental nucleus	+
Microcellular tegmental nucleus	+
Rhombencephalon	
Pontine nuclei	±
Reticulotegmental nuclei	
Reticular formation	
Central gray of the pons	+
Central gray, alpha part	+
Pontine reticular nucleus (oral and caudal part)	+
Rostroventrolateral reticular nucleus	+
Caudoventrolateral reticular nucleus	+
Gigantocellular reticular nucleus	+
Lateral paragigantocellular nucleus	+++
Dorsal paragigantocellular nucleus	++
Genu of the facial nerve	++
Accessory facial nucleus	+
Prepositus nucleus	+
Subcoeruleus nucleus, alpha part	+
Lateral reticular nucleus	+
Medullary reticular nucleus (dorsal & ventral part)	+
Nucleus of the solitary tract	+
Superior olivary complex	
Superior paraolivary nucleus	++
Nucleus of the trapezoid body	++
Cranial motor nuclei	
Motor trigeminal nucleus (dorsolateral & ventromedial part)	+++
Facial nucleus	++
Dorsal motor nucleus of vagus	++
Hypoglossal nucleus	++
Ambiguus nucleus	++
Sensory trigeminal nucleus	
Spinal trigeminal nucleus (oral & caudal part) [fibrous]	+
Spinal trigeminal tract [fibrous]	+
Cochlear nuclei	
Ventral cochlear nucleus	+
Vestibular nucleus	
Lateral vestibular nucleus	++
Medial vestibular nucleus	++
Superior vestibular nucleus	++
Precerebellar nucleus	
Inferior olive	+
Cerebellar cortex	
Purkinje cells	++
Cerebellar nuclei	
Lateral cerebellar nucleus	+
Superior cerebellar peduncle [fibrous]	+
Spinal cord	
Motor neurons	++
Substantia gelatinosa	+

Relative intensities of Lf-LI were estimated by visual comparison of immunolabeled slides: ±, faint; +, low; ++, moderate; +++, strong; ++++, very strong.

was undetectable by quantitative reverse transcription PCR in the mouse brain following transcardial perfusion with PBS (unpublished data). Yet, we observed varied levels of Lf mRNA expression in somatic organs in the same mice, with the highest levels in bone marrow. Therefore, we speculate that the neuronal Lf observed in this study was exogenously transported from the blood across the blood brain barrier. In the future, it would be helpful to examine in detail whether Lf is synthesized in the healthy CNS of young-adult mice.

The lack of an anti-mouse Lf antibody that is applicable to immunohistochemistry appears to have hampered studies on the role of Lf in various animal models of CNS disorders. This study provided such an antibody, and used it to reveal basic information on Lf distribution in the mouse CNS. The availability of a suitable anti-mouse Lf antibody is expected to encourage extensive studies on the roles of Lf in the healthy, aging, and neurodegenerating CNS.

Acknowledgments. This study was supported by JSPS KAKENHI Grant Numbers JP09770445 and JP18H02785. The authors would like to thank H. Kashiwai for excellent technical assistance.

References

1. Soerensen M and Soerensen SPL: The proteins in whey. CR Trav Lab Carlsberg (1939) 23: 55–99.
2. Schaefer KM: Untersuchungen zum Milcheiweiss Problem. Monatsschr Kinderheilkd (1951) 99: 66–71.
3. Masson PL, Heremans JF and Schonne E: Lactoferrin, an iron-binding protein in neutrophilic leukocytes. J Exp Med (1969) 130: 643–658.
4. Mazurier J and Spik G: Comparative study of the iron-binding properties of human transferrins. I. Complete and sequential iron saturation and desaturation of the lactotransferrin. Biochim Biophys Acta (1980) 629: 399–408.
5. Arnold RR, Cole MF and McGhee JR: A bactericidal effect for human lactoferrin. Science (1977) 197: 263–265.
6. Brinkmann V, Reichard U, Goosmann C, Fauler B, Uhlemann Y, Weiss DS, Weinrauch Y and Zychlinsky A: Neutrophil extracellular traps kill bacteria. Science (2004) 303: 1532–1535.
7. Brock J: Lactoferrin: a multifunctional immunoregulatory protein? Immunol Today (1995) 16: 417–419.
8. Baveye S, Elass E, Mazurier J, Spik G and Legrand D: Lactoferrin: a multifunctional glycoprotein involved in the modulation of the inflammatory process. Clin Chem Lab Med (1999) 37: 281–286.
9. Mariller C, Hardiville S, Hoedt E, Huvent I, Pina-Canseco S and Pierce A: Delta-lactoferrin, an intracellular lactoferrin isoform that acts as a transcription factor. Biochem Cell Biol (2012) 90: 307–319.
10. Shau H, Kim A and Golub SH: Modulation of natural killer and lymphokine-activated killer cell cytotoxicity by lactoferrin. J Leukoc Biol (1992) 51: 343–349.
11. Crouch SP, Slater KJ and Fletcher J: Regulation of cytokine release from mononuclear cells by the iron-binding protein lactoferrin. Blood (1992) 80: 235–240.
12. Mattsby-Baltzer I, Roseanu A, Motas C, Elverfors J, Engberg I and Hanson LA: Lactoferrin or a fragment thereof inhibits the endotoxin-induced interleukin-6 response in human monocytic cells. Pediatr Res (1996) 40: 257–262.
13. He J and Furmanski P: Sequence specificity and transcriptional activation in the binding of lactoferrin to DNA. Nature (1995) 373: 721–724.
14. Penco S, Pastorino S, Bianchi-Scarra G and Garre C: Lactoferrin down-modulates the activity of the granulocyte macrophage colony-stimulating factor promoter in interleukin-1 beta-stimulated cells. J Biol Chem (1995) 270: 12263–12268.
15. Leveugle B, Spik G, Perl DP, Bouras C, Fillit HM and Hof PR: The iron-binding protein lactotransferrin is present in pathologic lesions in a variety of neurodegenerative disorders: a comparative immunohistochemical analysis. Brain Res (1994) 650: 20–31.
16. Kawamata T, Tooyama I, Yamada T, Walker DG and McGeer PL: Lactotransferrin immunocytochemistry in Alzheimer and normal human brain. Am J Pathol (1993) 142: 1574–1585.
17. Leveugle B, Faucheux BA, Bouras C, Nillesse N, Spik G, Hirsch EC, Agid Y and Hof PR: Cellular distribution of the iron-binding protein lactotransferrin in the mesencephalon of Parkinson's disease cases. Acta Neuropathol (1996) 91: 566–572.
18. Day CL, Anderson BF, Tweedie JW and Baker EN: Structure of the recombinant N-terminal lobe of human lactoferrin at 2.0 A resolution. J Mol Biol (1993) 232: 1084–1100.
19. Kondo Y, Asanuma M, Nishibayashi S, Iwata E and Ogawa N: Late-onset lipid peroxidation and neuronal cell death following transient forebrain ischemia in rat brain. Brain Res (1997) 772: 37–44.
20. Kondo Y, Nakanishi T, Takigawa M and Ogawa N: Immunohistochemical localization of connective tissue growth factor in the rat central nervous system. Brain Res (1999) 834: 146–151.
21. Hof PR, Young WG, Bloom FE, Belichenko PV and Celio MR: Comparative cytoarchitectonic atlas of the C57BL/6 and 129/Sv mouse brains. 1st ed. Elsevier, Amsterdam (2000).
22. Pulsinelli WA, Brierley JB and Plum F: Temporal profile of neuronal damage in a model of transient forebrain ischemia. Ann Neurol (1982) 11: 491–498.
23. Britigan BE, Serody JS and Cohen MS: The role of lactoferrin as an anti-inflammatory molecule. Adv Exp Med Biol (1994) 357: 143–156.
24. Zheng JP, Xie YZ, Li F, Zhou Y, Qi LQ, Liu LB and Chen Z: Lactoferrin improves cognitive function and attenuates brain senescence in aged mice. Journal of Functional Foods (2020) 65: 103736.
25. Zimecki M, Kocieba M, Chodaczek G, Houszka M and Kruzel ML: Lactoferrin ameliorates symptoms of experimental encephalomyelitis in Lewis rats. J Neuroimmunol (2007) 182: 160–166.
26. Suzuki YA and Lonnerdal B: Baculovirus expression of mouse lactoferrin receptor and tissue distribution in the mouse. Biometals (2004) 17: 301–309.
27. Liu YH and Teng CT: Characterization of estrogen-responsive mouse lactoferrin promoter. J Biol Chem (1991) 266: 21880–21885.
28. Pentecost BT and Teng CT: Lactotransferrin is the major estrogen inducible protein of mouse uterine secretions. J Biol Chem (1987) 262: 10134–10139.

29. Benson S: Hormone replacement therapy and Alzheimer's disease: an update on the issues. Health Care Women Int (1999) 20: 619–638.
30. Monk D and Brodaty H: Use of estrogens for the prevention and treatment of Alzheimer's disease. Dement Geriatr Cogn Disord (2000) 11: 1–10.
31. Vogel HJ: Lactoferrin, a bird's eye view. Biochem Cell Biol (2012) 90: 233–244.
32. Gholkar AA, Schmollinger S, Velasquez EF, Lo YC, Cohn W, Capri J, Dharmarajan H, Deardorff WJ, Gao LW, Abdusamad M, Whitelegge JP and Torres JZ: Regulation of Iron Homeostasis through Parkin-Mediated Lactoferrin Ubiquitylation. Biochemistry (2020) 59: 2916–2921.
33. Rousseau E, Michel PP and Hirsch EC: The iron-binding protein lactoferrin protects vulnerable dopamine neurons from degeneration by preserving mitochondrial calcium homeostasis. Mol Pharmacol (2013) 84: 888–898.
34. Mazurier J, Legrand D, Hu WL, Montreuil J and Spik G: Expression of human lactotransferrin receptors in phytohemagglutinin-stimulated human peripheral blood lymphocytes. Isolation of the receptors by antiligand-affinity chromatography. Eur J Biochem (1989) 179: 481–487.
35. Leveugle B, Mazurier J, Legrand D, Mazurier C, Montreuil J and Spik G: Lactotransferrin binding to its platelet receptor inhibits platelet aggregation. Eur J Biochem (1993) 213: 1205–1211.
36. Hu WL, Mazurier J, Sawatzki G, Montreuil J and Spik G: Lactotransferrin receptor of mouse small-intestinal brush border. Binding characteristics of membrane-bound and triton X-100-solubilized forms. Biochem J (1988) 249: 435–441.
37. Rochard E, Legrand D, Lecocq M, Hamelin R, Crepin M, Montreuil J and Spik G: Characterization of lactotransferrin receptor in epithelial cell lines from non-malignant human breast, benign mastopathies and breast carcinomas. Anticancer Res (1992) 12: 2047–2051.
38. Fillebeen C, Descamps L, Dehouck MP, Fenart L, Benaissa M, Spik G, Cecchelli R and Pierce A: Receptor-mediated transcytosis of lactoferrin through the blood-brain barrier. J Biol Chem (1999) 274: 7011–7017.
39. Huang RQ, Ke WL, Qu YH, Zhu JH, Pei YY and Jiang C: Characterization of lactoferrin receptor in brain endothelial capillary cells and mouse brain. J Biomed Sci (2007) 14: 121–128.
40. Fillebeen C, Dehouck B, Benaissa M, Dhennin-Duthille I, Cecchelli R and Pierce A: Tumor necrosis factor-alpha increases lactoferrin transcytosis through the blood-brain barrier. J Neurochem (1999) 73: 2491–2500.
41. Fillebeen C, Mitchell V, Dexter D, Benaissa M, Beauvillain J, Spik G and Pierce A: Lactoferrin is synthesized by mouse brain tissue and its expression is enhanced after MPTP treatment. Mol Brain Res (1999) 72: 183–194.
42. Fillebeen C, Ruchoux MM, Mitchell V, Vincent S, Benaissa M and Pierce A: Lactoferrin is synthesized by activated microglia in the human substantia nigra and its synthesis by the human microglial CHME cell line is upregulated by tumor necrosis factor alpha or 1-methyl-4-phenylpyridinium treatment. Mol Brain Res (2001) 96: 103–113.